Compact Lunar Mineralogy Imager (CLuMI). S. Aslam[1] (shahid.aslam-1@nasa.gov), D. Bower[2,1], F. Cepollina[3,1], T. Flatley[4,1], T. Hewagama[2,1], D. Jennings[5], M. Jhabvala[1], and T. A. Livengood[2,1], [1]NASA Goddard Space Flight Center, Code 693, Greenbelt, MD 20771, [2]Department of Astronomy, University of Maryland, College Park, MD 20742, [3]Conceptual Analytics, LLC, Glenn Dale, MD 20769, [4]Genesis Engineering Solutions, Inc., Lanham, MD 20706, [5]Space Systems and Applications, Inc., Lanham, MD 20706.

Introduction: Compact Lunar Mineralogy Imager (CLuMI) is a MWIR/LWIR hyperspectral imager (Fig. 1) to identify and characterize lunar materials and ice(s) on surface and walls from 1-5 meters standoff distance. The measurements support the decadal survey priority science goal of dating surface material using spectral imagery to identify stratification and exposed materials and provide "geology of the South-Pole Aitken basin" [1]. CLuMI is relevant to planning of in situ resource utilization (ISRU) operations, including mineral and water extraction. NASA has identified the lunar south polar region as a human landing and exploration site. This region contains water and is rich in minerals of significance for ISRU. While a new generation of innovative missions, including SmallSat, are expected to map composition on a global scale (*e.g.*, Lunar IceCube, Lunar Flashlight, Korean Lunar Pathfinder Orbiter), extraction on a scale viable for use by astronauts and mission operations will require mapping resources on finer scales, including vertical surfaces and permanently shadowed regions (PSRs) not exposed to spacecraft observations.

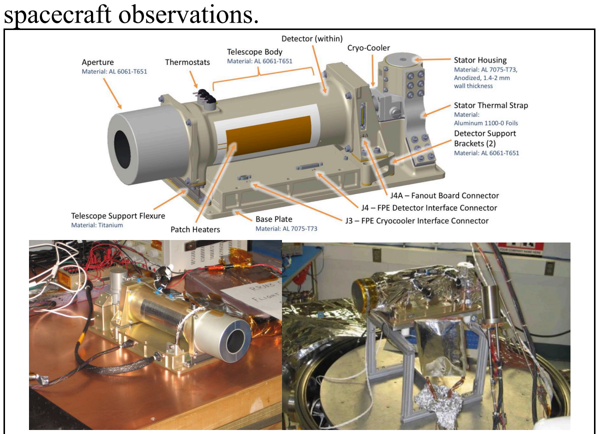

Figure 1: CLuMI, based on CTI instrumentation developed at GSFC, incorporates a broadband, sensitive quantum detector coupled with a linear variable filter in a compact profile.

In addition to rover based robotic exploration, measurement by field astronauts is a critical next step that optimizes mining operations. CLuMI is designed for use by astronauts in an automated, efficient manner and assures safety of personnel and equipment as a standoff survey instrument. For example, optical sensing from a distance enables an astronaut to rapidly explore composition in a survey mode and peruse difficult to access terrains from a safe distance.

Science Background: Identification of lunar rock forming minerals (ilmenite, plagioclase, pyroxene, spinel, olivine, armalcolite), accessory minerals (*e.g.*, feldspar, and apatite), and trace minerals (*e.g.*, silicates, sulfides/sulfates) will guide requirements for mining instrumentation. Fig. 2 shows the 2-12 µm spectral signatures of pure samples of these materials and sets spectroscopic requirements for CLuMI in terms of species separation.

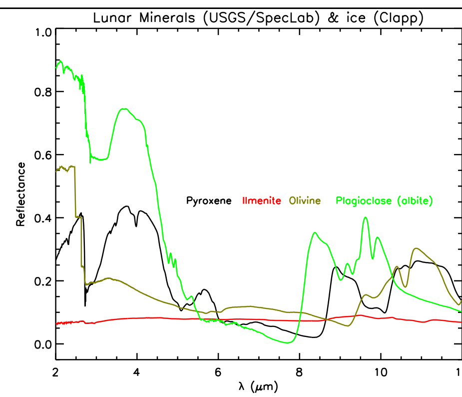

Figure 2: Representative spectral signature of four prominent lunar mineral type (extracted from USGS Spectral Library [9]).

Recent studies suggest significant water deposits are possible in cold traps (~100 billion metric tons) [2][3]. The common optical sensing technology is based on the 3 µm (~3200-3700 cm^{-1}, stretching-modes) vibrational bands associated with both water (ν_1/ν_3) and OH (ν_1) [4]. In an analysis of lunar equatorial soils concluded solar-wind produced OH was a viable source for water ice in polar cold-traps with slower degassing rates [5]. Discrimination of water from OH bearing minerals is critical for planning of mining operations. The 6 µm (1595 cm^{-1}, ν_2 bending-mode vibrational band) of monomer ice (*e.g.*, I_h state) results in an emissivity peak [6] unique to water (from OH) and also seen in dirty ice [7]. One more signature of interest is the 12 µm (780 cm^{-1} libration) band. For thermal observations, control of the viewing (emission) angle is relevant given the angular dependence of emissivity [8]. Combined with the 3 µm and 12 µm signatures, an instrument capable of sensing these bands will detect and distinguish water ice from OH in the matrix. Calibration of broadband thermal signatures will provide temperatures for context.

Instrument Design: CLuMI is a 2-12 µm hyperspectral imaging camera with a sensitive 1 Mpixel Stained Layer Superlattice (SLS) cooled quantum detector coupled with a linear variable filter (LVF), a cross section of the instrument is shown in Fig. 3. The Compact Thermal Imager (CTI) is the heritage instrument on which CLuMI is based [10]. CTI was deployed on the International Space Station as part of the Remote Robotic Mission 3 (RRM3). CTI successfully observed biomass combustion. As with CTI, CLuMI also has a small form-factor (2.5 U), low-mass (2 kg), low-power (12 W peak), and incorporates a focal plane integrated assembly of linear variable and discrete filters. Focal plane integration controls light scattering by external free space optics, and results in a compact instrument. Since the filter assembly will relax to the focal planet temperature, thermal emission from the cold filters are minimal compared to an external filter. The system integrates an infrared lamp to illuminate dark regions of interest. The spectral response of the SLS sensor brackets the spectral signatures of ISRU-relevant compounds. A compact broadband visible imager boresighted with the infared sensor will provide contextual images of the region being investigated. Integrated electronics control the instruments, provides storage, and functions as a user interface.

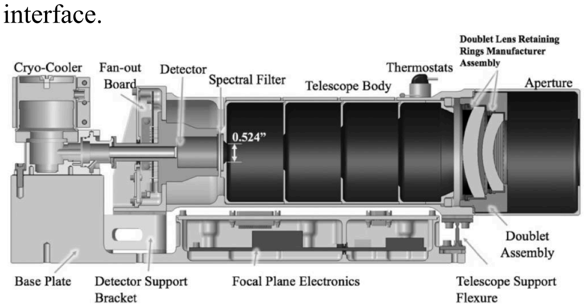

Figure 3: Cross-sectional view of CLuMI showing locations of cryo-cooler, detectors and spectral filters. Assembly is 400 mm x 150 mm x 150 mm.

Measurement methodology: The instrument will scan the area, perform automated analysis, flag minerals of interest, save data to storage, and indicate importance of region to astronaut with LED based feedback. The LVF requires pushbroom scanning to acquire hyperspectral maps of the scene of interest. We envision the following operational scenario. An astronaut will transport CLuMI by hand or in a rover (Fig. 4). When a desired region is encountered, the astronaut will deploy the instrument on a tripod, and use a visible camera to orient and point the instrument. A single button initiates frame capture. The instrument is on a stepper motor mechanism that scans the region of interest so that the extent of the LVF slides over the region. The frame sequence is written to a solid-state storage unit for detailed analysis at the base station or for Earth telemetry. On board processing software compares the acquired spectra to a table of relevant spectra. If a match is found, then the instrument triggers immediate feedback to the astronaut. The additional functionality will enable the astronaut to characterize the region is more detail as needed.

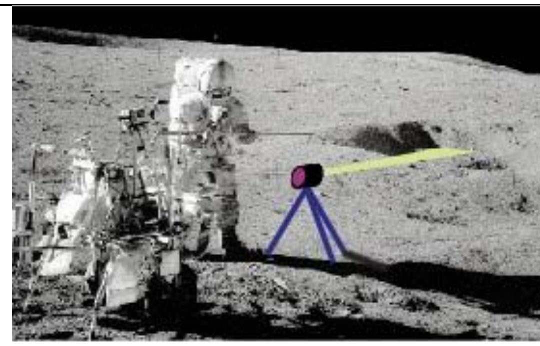

Figure 4: CLuMI on a tripod will image a region of interest at a distance, permitting the astronaut to characterize permanently shadowed regions at a safe range. CLUMI can also be mounted on a lunar lander deck.

Acknowledgments: We acknowledge GSFC internal R&D funds that enabled early work.

References: [1] NASA’s Strategic Plan for Lunar Exploration (2016). [2] Ruanenko L., Venkatraman J., and Paige D.A. (2019) *Nat. Geosci*., *12*, 597-601. [2] Rashid T., Khawaja H.A., and Edvardsen K. (2015) *Sensor Comm., Ninth International Conf. on Sensor Technologies and Applications*. [3] Li S., Lucey P. G., Milliken R. E., Hayne P.O., Fisher E., Williams J-P., Hurley D. M., and Elphic C. (2020) *PNAS, 115,* 8907-8912. [4] Bandfield J. L., Poston M. J., Klima R. L., and Edwards C. S. (2018) *Nat. Geosci., 11,* 173-177. [5] Liu Y., Guan Y., Zhang Y., Rossman G.R, Eiler J. M., Taylor L. A. (2012) *Nat. Geosci., 5*, 779-782. [6] Warren S. G. and Brandt R. E. (2008) *J.G.R., 113,* D14220. [7] Ehrenfreund P., Gerkines P. A., Schutte W. A., van Hemert M. C., and van Dishoeck E. F. (1996) *Astr. AstrPhy., 312,* 263-274. [8] Warren T. J., Bowles N. E., Hanna K. D., and Bandfield J. L. (2019) *J.G.R Planets, 124,* 585-601. [9] Kokaly R. F., Clark R. N., Swayze G. A. (2017) USGS Spectral Library Version 7, U.S. Geological Survey Data Series 1035, 61. (2016). [10] Jhabvala M., Jennings D., Tucker C. *et al*. (2019) *Applied Optics, 58,* 5432-5442.